

STUDY OF AN INTERMEDIATE AGE OPEN CLUSTER IC 1434 USING GROUND-BASED IMAGING AND GAIA DR2 ASTROMETRY

Y.H.M. Hendy,¹ and D. Bisht^{*2}

Draft version: June 15, 2021

RESUMEN

ABSTRACT

We present a detailed photometric and kinematical analysis of poorly studied open cluster IC 1434 using CCD VRI, APASS, and Gaia DR2 database for the first time. By determining the membership probability of stars, we identified the 238 most probable members with a probability higher than 60% by using proper motion and parallax data as taken from the Gaia DR2 catalog. The mean proper motion of the cluster is obtained as $\mu_x = -3.89 \pm 0.19$ and $\mu_y = -3.34 \pm 0.19$ mas yr⁻¹ in both the directions of right ascension and declination. The radial distribution of member stars provides cluster extent as 7.6 arcmin. We have estimated the interstellar reddening ($E(B-V)$) as 0.34 mag using the transformation equations from literature. We obtained the values of cluster age and distance are 631 ± 73 Myr and 3.2 ± 0.1 Kpc.

Key Words: Open star cluster IC 1434 — Color Magnitude Diagram — Astrometry

1. INTRODUCTION

Open clusters (OCs) are important tools to probe the Galactic disk properties (see, e.g., Friel 1995). OCs are very advantageous to interpret many queries regarding the assessment of chemical abundance gradients in the disk (see, e.g., Twarog, Ashman & Anthony-Twarog 1997; Chen, Hou & Wang 2003), Galactic structure and evolution (e.g., Janes & Adler 1982; Janes & Phelps 1994), interactions between thin and thick disks (e.g., Sandage 1988), as well as the theories of stellar formation and evolution (e.g., Meynet, Mermilliod & Maeder 1993; Phelps & Janes 1993). It's not an easy task to segregate cluster members from field stars considering OCs are generally projected against the Galactic disc stars. The second data release (DR2) (Gaia Collaboration et al. 2016a) contains 1.7 billion sources and was made public on 2018 April 24 (Jordi et al. 2010; Gaia Collaboration et al. 2016a,b; Salgado et al. 2017). The Gaia DR2 data contains photometric magnitudes in three bands (G , G_{BP} , and G_{RP}) and astrometric data at the sub-milliarcsecond

¹Astronomy Department, National Research Institute of Astronomy and Geophysics (NRIAG), Helwan, Cairo, Egypt.

²Key Laboratory for Researches in Galaxies and Cosmology, University of Science and Technology of China, Chinese Academy of Sciences, Hefei, Anhui, 230026, China.

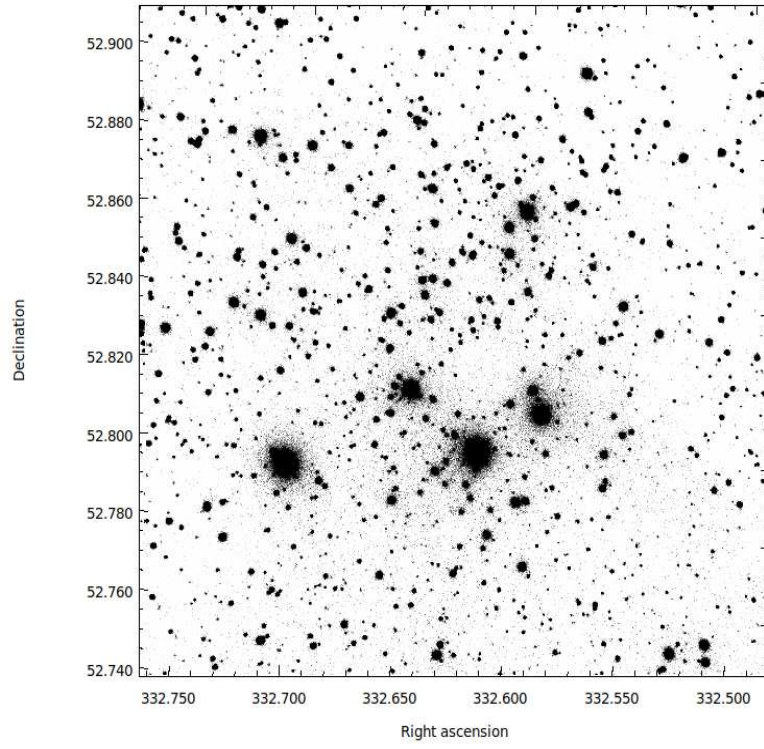


Fig. 1. Finding chart of the stars in the field of IC 1434. Filled circles of different sizes represent the brightness of the stars. The smallest size denotes stars of $V \sim 20$ mag.

level along with the parallax (Gaia Collaboration et al. 2018a). Gaia data has been used recently by many authors to estimate the membership probability of stars lying towards the cluster regions (Cantat-Gaudin et al. 2018; Gao 2018; Rangwal et al. 2019; Bisht et al. (2019, 2020a, 2020b)).

The open cluster IC 1434 ($\alpha_{2000} = 22^h 10^m 30^s$, $\delta_{2000} = 52^\circ 50' 00''$; $l=99^\circ.937$, $b=-2^\circ.700$) is located in the second Galactic quadrant. Tadross (2009) analyzed this object using 2MASS and NOMAD data sets. He obtained the age, interstellar reddening ($E(B - V)$), and distance of this object as 0.32 Gyr, 0.66 mag, and 3035 ± 140 pc, respectively. In this paper, our main goal is to accomplish a deep and precise analysis of an intermediate-age open cluster IC 1434 using CCD *VRI*, APASS, and Gaia DR2 data.

The layout of the paper is as follows. A brief description of data used, data reduction, and calibration are described in Section 2. Section 3 deals with the study of proper motion and determination of membership probability of stars. The structural properties and derivation of fundamental parameters using the most probable cluster members have been carried out in Section 4. The conclusions are presented in Section 5.

2. OBSERVATIONS AND CALIBRATION OF CCD DATA

The *VRI* CCD photometric observations of IC 1434 was carried out using the 74-inch Kottamia astronomical observatory (KAO) of NRIAG in Egypt. Images were collected using a $2k \times 2k$ CCD system. The observations were taken at the Newtonian focus with a field area of $10' \times 10'$ and a pixel scale of $0''.305 \text{ pixel}^{-1}$ on 8th November 2013. The read-out noise was $3.9 \text{ e}^-/\text{pixel}$. Observations were organized in several short exposures with the air mass ranges of 1.32-1.62 in each of the filter as described in Table 1. All CCD frames observed with two amplifiers, which treated for overscan, bias, and flat field corrections using an IRAF's code written by one of the authors (Y.H.M. Hendy), see Tadross et al. (2018). To perform the photometry, we have used a DAOPHOT package on IRAF (Stetson 1987, 1992). The data reduction procedure has been well explained by Bisht et al. (2019). The identification chart for IC 1434 based on our *V*-band observations is shown in Fig. 1.

To obtain the instrumental magnitudes of stars in the observed field, we used the point spread function of Stetson (1987). We have transformed the pixel coordinates (X and Y) into the right ascension and declination using the astrometry website (<https://nova.astrometry.net/>).

To transform the *VRI* instrumental magnitudes into Johnson and Kron-Cousin standard magnitudes, we have used the photometric data available in *V*-band from Maciejewski & Niedzielski (2008) and *RI*-bands from the USNO-B1.0 catalog (Monet et al. 2003).

The transformation equations for converting the instrumental magnitude in to standard magnitude, are as follows:

$$V = V_{ins} - (0.14 \pm 0.039)(V - R) + 21.18 \pm 0.031$$

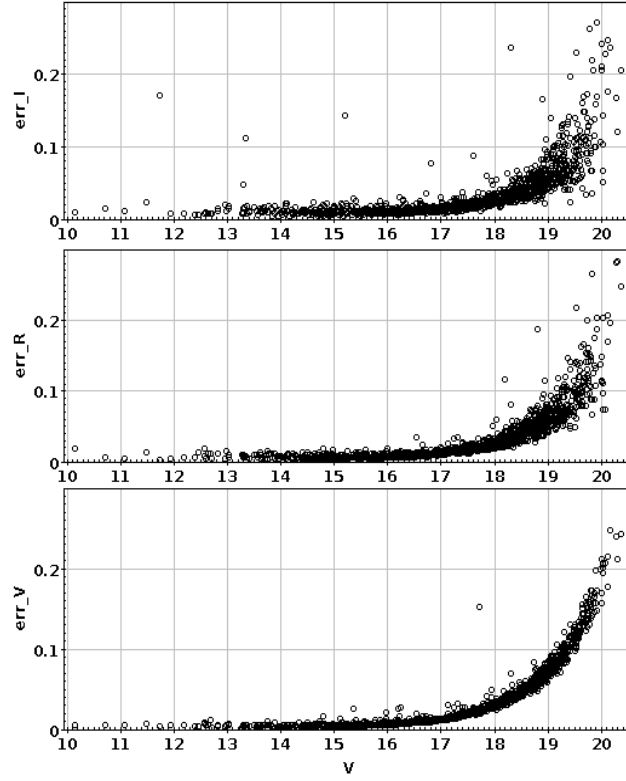


Fig. 2. Photometric errors in V , R , and I bands against V magnitude.

TABLE 1
LOG OF OBSERVATIONS, WITH DATES AND EXPOSURE TIMES
FOR EACH PASSBAND.

Band	Exposure Time (in seconds)	Date
V	$120 \times 3, 60 \times 1$	8 th November 2013
R	$120 \times 2, 60 \times 1$,,
I	$120 \times 3, 60 \times 1$,,

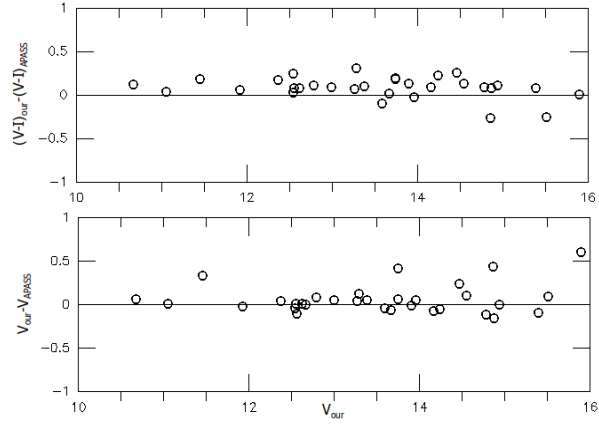


Fig. 3. Differences between measurements presented in the APASS catalog and this study for V magnitude and $(V-I)$ colors. Zero difference is indicated by the solid line

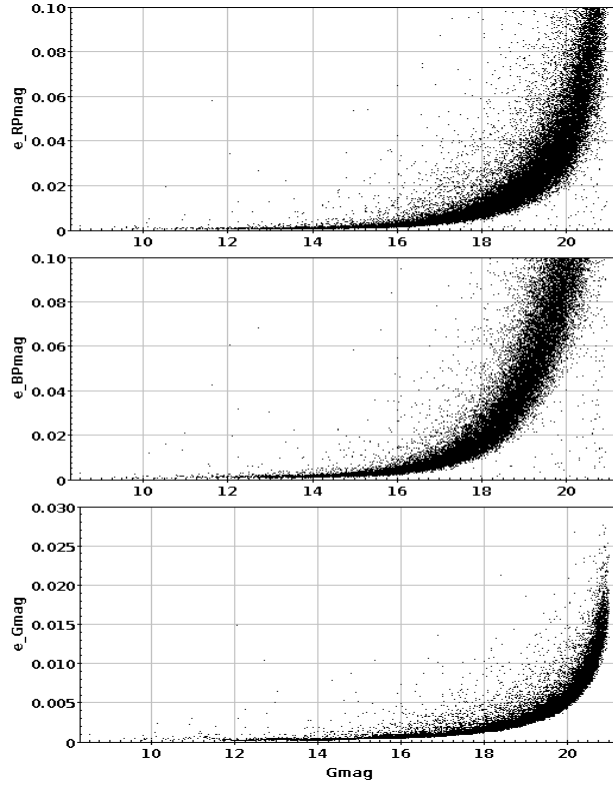


Fig. 4. Photometric errors in Gaia bands (G , BP , and RP) against G magnitude.

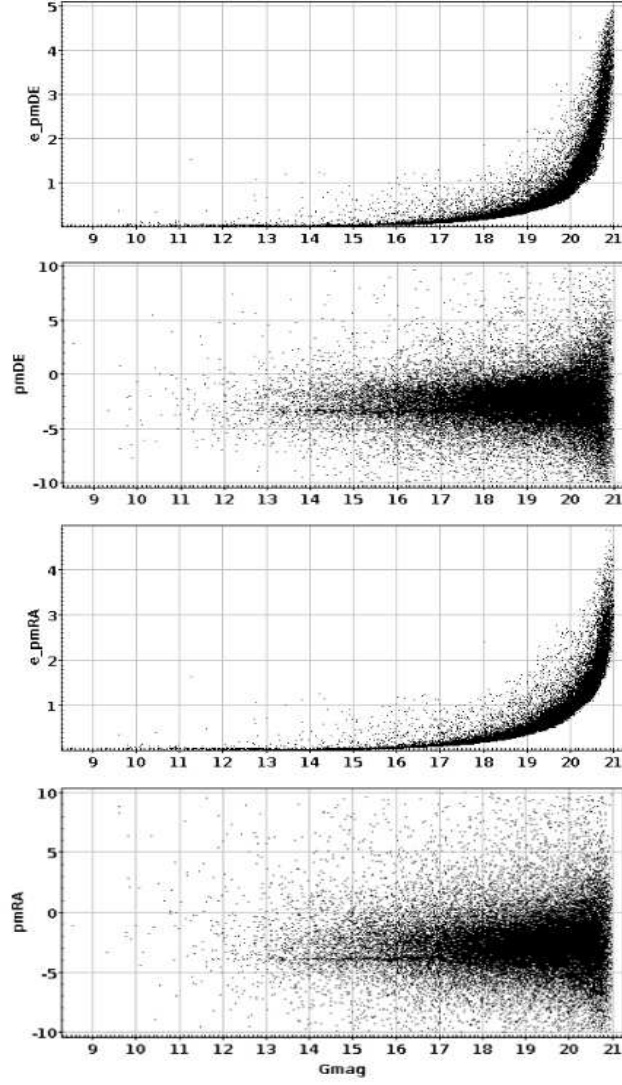


Fig. 5. The plot of proper motions and their errors versus G magnitude.

$$\begin{aligned}
V - R &= (1.06 \pm 0.035)(V - R)_{ins} + 0.56 \pm 0.022 \\
V - I &= (0.90 \pm 0.036)(V - I)_{ins} + 0.85 \pm 0.027
\end{aligned}$$

The respective errors in zero points and color coefficients are ~ 0.03 mag shown in the above transformation equations. The internal errors derived from DAOPHOT are plotted against V magnitude shown in Fig. 2. This figure shows that the average photometric errors are ≤ 0.02 mag at $V \sim 18^{th}$ mag, while it is ≤ 0.1 mag at $V \sim 19^{th}$ mag.

To compare the photometry, we have cross-identified the stars in our observed data with the American Association of Variable Star Observers (AAVSO) Photometric All-Sky Survey (APASS) DR9 catalog. We have assumed that stars are accurately matched if the difference in position is less than 1 arcsec and in this way, we have found 32 common stars accordingly. The APASS survey is cataloged in five filters B , V , g , r , and i . The range of magnitude in the V band is from 7 to 17 mag (Heden & Munari 2014). The DR9 catalog covers almost about 99 % of the sky (Heden et al. 2016). To obtain the Cousins I band using Sloan ri photometric bands from the APASS catalog ($I_{APASS} = i - (0.337 \pm 0.191) (r - i) - (0.370 \pm 0.041)$), we have adopted the method given by Tadross & Hendy (2016).

The difference indicates that present V and $(V-I)$ measurements are in fair agreement with those stars given in the APASS catalog. The comparable difference is found as 0.07 in the V band and 0.08 in $(V-I)$ as shown in Fig. 3.

2.1. Gaia DR2

Gaia DR2 (Gaia Collaboration et al. 2018b) database within a $20'$ radius of the cluster is used for the astrometric analysis. This data consists of positions on the sky (α, δ), parallaxes and proper motions ($\mu_\alpha \cos \delta, \mu_\delta$) with a limiting magnitude of $G = 21$ mag. The errors in photometric magnitudes (G , G_{BP} , and G_{RP}) with G mag are shown in Fig 4. In this figure, we find the mean errors in G the band is ~ 0.01 mag while the mean errors in G_{BP} and G_{RP} bands are ~ 0.1 mag at 20 mag. The proper motions with their respective errors are plotted against G magnitude is shown in Fig. 5. The uncertainties in the corresponding proper motion components are ~ 0.06 mas yr^{-1} (for $G \leq 15$ mag), ~ 0.2 mas yr^{-1} (for $G \sim 17$ mag), and ~ 1.2 mas yr^{-1} (for $G \sim 20$ mag).

3. PROPER MOTION STUDY AND MEMBERSHIP PROBABILITIES OF STARS

The proper motion of a cluster is a change in its angular position with time as seen from the center of mass of the solar system. Proper motions play an influential role to eliminate non-members from the cluster's main sequence (Yadav et al. 2013; Bisht et al. 2020a). We have cross-matched

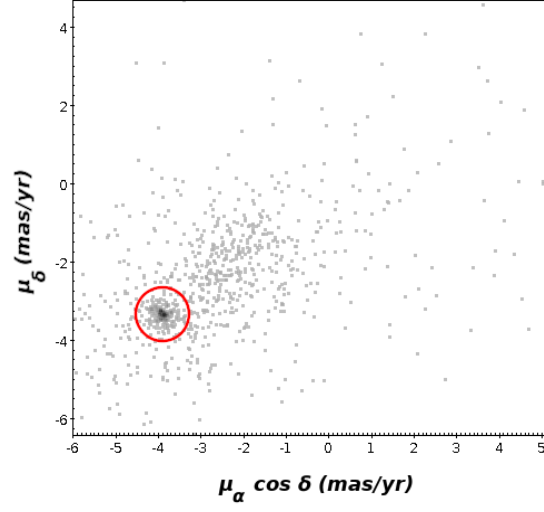


Fig. 6. Vector point diagram, circle defines the cluster region of IC 1434 within the radius of 0.6 mas/yr.

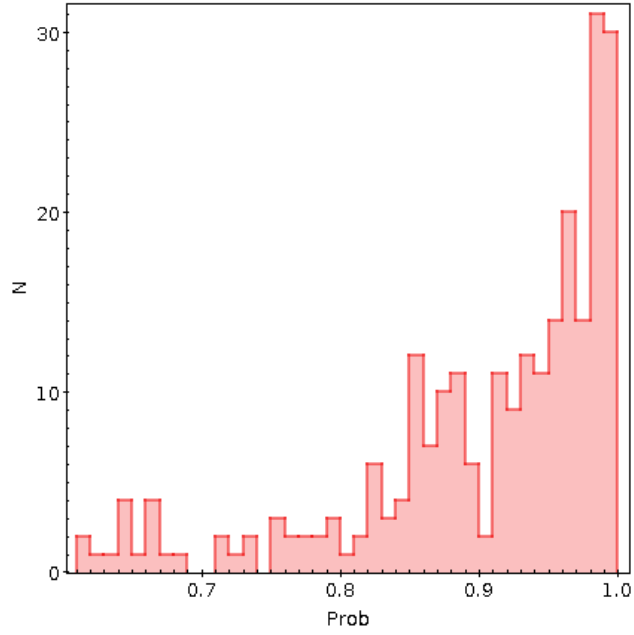


Fig. 7. A membership probability histogram of stars for IC 1434. We considered stars with a probability ≥ 0.6 as cluster members.

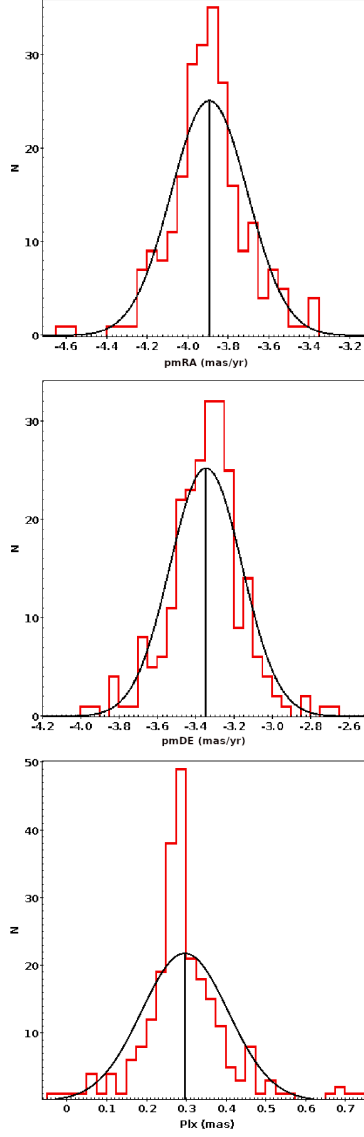


Fig. 8. Histogram to determine mean values of proper motions in RA and DEC directions (top and middle panels). Histogram to find mean parallax (bottom panel). The Gaussian function fits to the central bins provide the mean values in PMs and parallax shown in each panel.

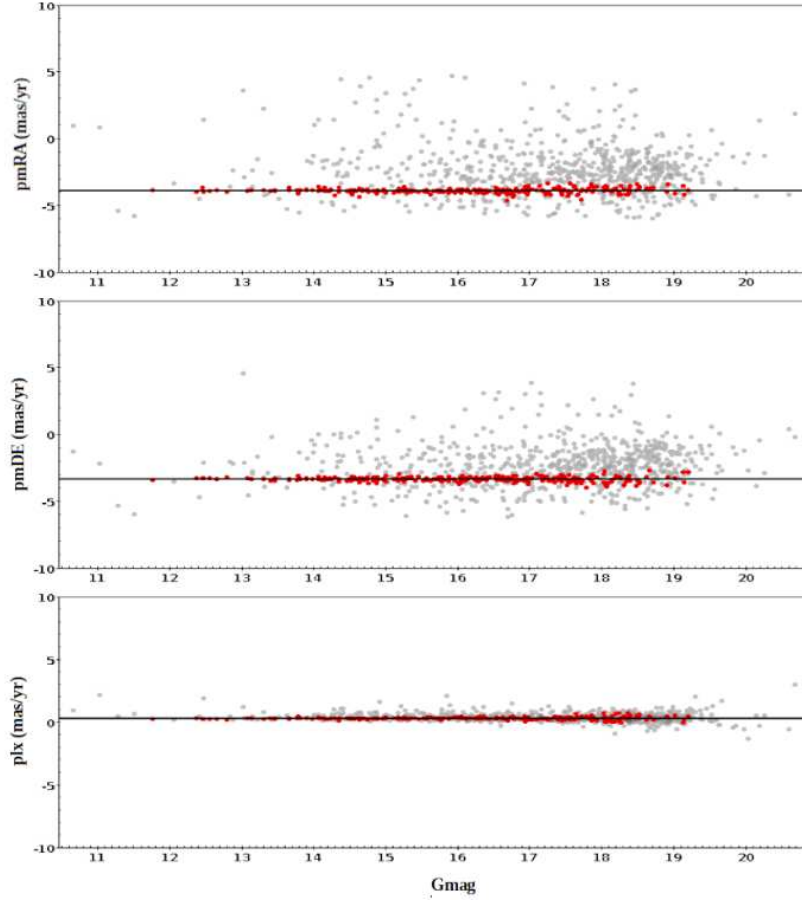


Fig. 9. Proper motion components and parallax distribution of most probable members (red dots) & all stars (gray dots) against G band magnitude. The horizontal line indicates the mean value of PMs and parallax.

our observational data in VRI bands and data from the Gaia DR2 catalog. A circle of 0.6 mas/yr around the cluster center in the VPD characterizes our membership criteria as shown in Fig. 6. The chosen radius in VPD is a compromise between losing members with poor proper motions and the inclusion of field region stars.

The OCs are highly contaminated by a large number of foreground/background stars especially towards the fainter end of the main sequence. Vasilevskis et al. (1958) have set up a mathematical model to obtain membership probabilities of stars using proper motion data. A revised technique was developed by Stetson (1980) and Zhao & He (1990) to check the membership of stars in OCs based on proper motions. To find the membership probability of stars towards the region of IC 1434, we have adopted the criteria as discussed by Kharchenko et al. (2004). This method has been previously used by Bisht et al. (2018) for OCs Teutsch 10 and Teutsch 25. Hendy (2018) also has been used this method for open cluster FSR 814. The kinematical probability of stars is expressed as:

$$p_k = e^{[-0.25(\frac{(\mu_x - \overline{\mu_x})^2}{\sigma_x^2} + \frac{(\mu_y - \overline{\mu_y})^2}{\sigma_y^2})]}$$

where $\sigma_x^2 = \sigma_{\mu_x}^2 + \sigma_{\overline{\mu_x}}^2$ and $\sigma_y^2 = \sigma_{\mu_y}^2 + \sigma_{\overline{\mu_y}}^2$. Here μ_x and μ_y are the proper motion of a particular star, while σ_{μ_x} and σ_{μ_y} are the corresponding errors. The $\overline{\mu_x}$ and $\overline{\mu_y}$ are the mean value of proper motions, while $\sigma_{\overline{\mu_x}}$ and $\sigma_{\overline{\mu_y}}$ are their corresponding standard deviations. Using the above method, we have identified possible members of IC1434 if the membership probability of stars higher than 60% which can be seen in Fig. 7.

We have used only probable cluster members to estimate the mean value of proper motions and parallax of IC 1434. We have fitted Gaussian profile to the construct histograms shown in Fig. 8. We obtained the mean-proper motion of IC 1434 -3.89 ± 0.19 and $-3.34 \pm 0.19 \text{ mas yr}^{-1}$ in RA and DEC directions, respectively. We determined the mean value of parallax $0.30 \pm 0.11 \text{ mas}$. Our findings are very close with the values given by Cantat-Gaudin et al. (2018).

Finally, we have considered a star as the most probable member if it lies within 0.6 mas/yr radius in VPD, having a membership probability higher than 60% and a parallax within 3σ from the mean parallax of the cluster IC 1434. In Fig. 9, we have plotted the proper motions and parallax distribution of most probable members as denoted by red dots & all observed stars as denoted by gray dots against G magnitude. In this figure, the horizontal solid line indicates the mean value of proper motions and parallax.

4. STRUCTURAL PROPERTIES OF IC 1434

4.1. *Spatial structure:radial density profile*

The accuracy of central coordinates is very important for the reliable estimation of the cluster's main fundamental parameters (e.g., age, distance,

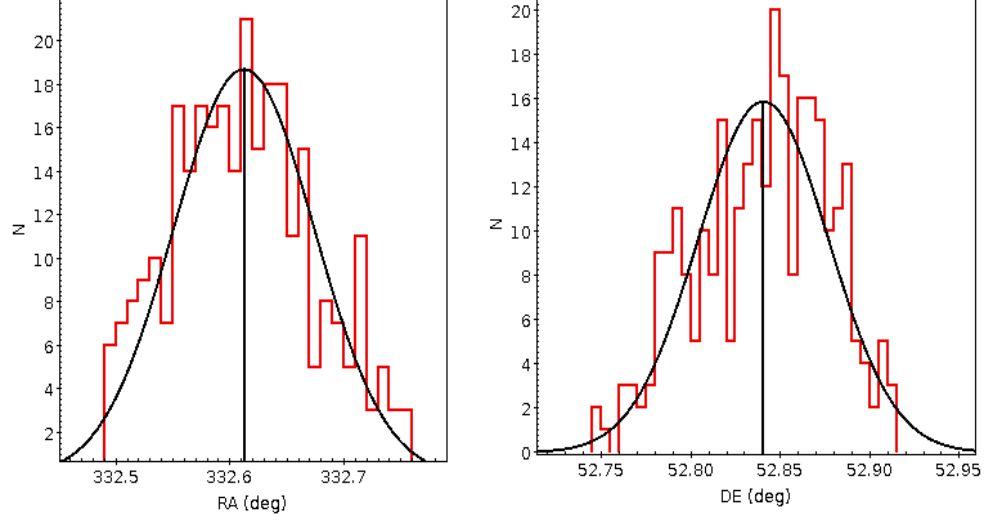


Fig. 10. Profiles of stellar counts across cluster IC 1434. The Gaussian fits have been applied. The center of symmetry about the peaks of Right Ascension and Declination is taken to be the position of the cluster centers.

reddening, etc.). We applied a star-count technique to obtain the center coordinates towards the area of IC 1434. The resulting histograms in both the RA and DEC directions are shown in the left panel of Fig. 10. The Gaussian curve-fitting at the central zones provides the center coordinates as $\alpha = 332.612 \pm 0.06$ deg ($22^h 10^m 26.8^s$) and $\delta = 52.84 \pm 0.04$ deg ($52^\circ 50' 24''$). These estimated values are in very good agreement with the values given by Dias et al. (2002) and Cantat-Gaudin et al. (2018).

Radial density profile (RDP) has been plotted in Fig. 11 to estimate the radius of the cluster. We divided the observed area of IC 1434 into several concentric rings. The number density, R_i , in the i^{th} zone is determined by using the formula $R_i = \frac{N_i}{A_i}$, where N_i is the number of stars and A_i is the area of the i^{th} zone. This RDP flattens at $R \sim 7.6$ arcmin and begins to merge with the background density as clearly shown in the right panel of Fig. 11. Therefore, we consider 7.6 arcmin as the cluster radius. A smooth continuous line represents the fitted King (1962) profile:

$$f(r) = f_{bg} + \frac{f_0}{1+(r/r_c)^2}$$

where r_c , f_0 , and f_{bg} are the core radius, central density, and the background density level, respectively. By fitting the King model to RDP, we estimated the structural parameters of IC 1434 are listed in Table 2.

We have estimated the concentration parameter using equation $c = \log(\frac{r_{lim}}{r_c})$, as given by Peterson & King (1975). In the present study, the concentra-

TABLE 2

STRUCTURAL PARAMETERS OF IC 1434. BACKGROUND AND CENTRAL DENSITY IS IN THE UNIT OF STARS PER ARCMIN². CORE RADIUS (R_c) IS IN ARCMIN.

Name	f_0	f_b	R_c	c	δ_c
IC 1434	23.70 ± 3.49	8.78 ± 0.21	1.25 ± 0.19	0.78	3.7

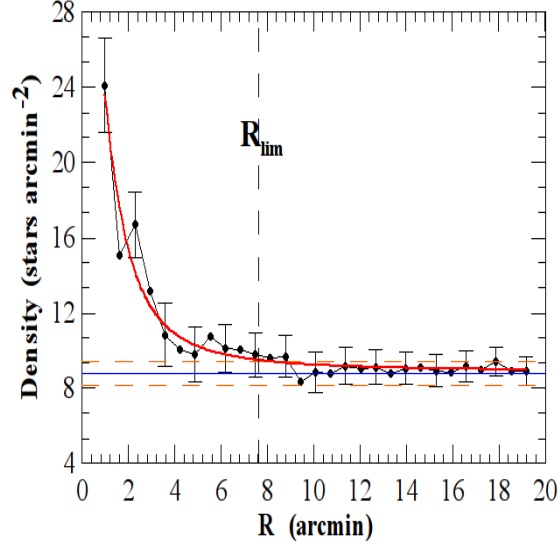


Fig. 11. Surface density distribution of the cluster IC 1434. Errors are determined from sampling statistics $\frac{1}{\sqrt{N}}$, where N is the number of stars used in the density estimation at that point. The smooth line represents the fitted profile whereas the dotted line shows the background density level. Long and short dash lines represent the errors in background density.

tion parameter is found to be 0.78 for IC 1434. Maciejewski & Niedzielski (2007) reported that R_{lim} may vary for individual clusters from $2R_c$ to $7R_c$. The estimated value of R_{lim} ($\sim 6.1R_c$) shows a fair agreement with the Maciejewski & Niedzielski (2007). We obtained the density contrast parameter ($\delta_c = 1 + (f_0/f_{bg})$) for IC 1434 as 3.7. It is lower than $7 \leq \delta_c \leq 23$ as derived by Bonatto & Bica (2009). This demonstrates that IC 1434 is a sparse cluster.

4.2. Age and distance estimation using CMD

Age and distance are important parameters to trace the structure and chemical evolution of the Milky Way Galaxy using OCs (Friel & Janes 1993). The $(G, BP - RP)$, and $(V, V - I)$ color magnitude diagrams (CMDs) are shown in Fig. 12. In this figure, filled dots are the most probable cluster members with membership probability $\geq 60\%$ while open circles are matched ones with the catalog given by Cantat-Gaudin et al. (2018). The age of IC 1434 has been estimated by fitting the theoretical isochrones of Marigo et al. (2017) with metallicity of $Z = 0.0152$ to the CMDs as shown in Fig. 12. In this figure, we used the isochrones of different ages of $\log(\text{age}) = (8.75, 8.80 \text{ and } 8.85)$. We found the best global fit at $\log(\text{age})=8.80$, which is corresponding to 631 ± 73 Myr of cluster's age.

Our estimated value of color-excess in Gaia bands ($E(BP - RP)$) is 0.43 mag from the isochrones fitting to the CMD's. We have calculated the interstellar reddening ($E(B - V)$) as 0.34 mag using the transformation equations ($E(B - V) = 0.785 E(BP - RP)$) as taken from Abdelaziz et al. (2020). Distance modulus ($m - M_G = 12.51$ mag) of IC 1434 provides the heliocentric distance as 3.2 ± 0.1 kpc. Our estimated values of $E(B - V)$ and distance modulus are in fair agreement with the values $E(B - V) = 0.49$ and $m - M_G = 12.43$ as obtained by Angelo et al. (2020).

We obtained the Galactocentric distance as 9.4 ± 0.1 kpc by assuming 8.3 kpc distance of the Sun to the Galactic center. The Galactocentric coordinates are estimated as $X_\odot = -0.55 \pm 0.04$ kpc, $Y_\odot = 3.1 \pm 0.2$ kpc and $Z_\odot = -0.15 \pm 0.010$ kpc. The estimated values of Galactocentric coordinates are very close to the values obtained by Cantat-Gaudin et al. (2018).

We also have checked the distance of IC 1434 using a parallax of stars from the Gaia DR2 catalog. We found the distance of this object as 3.3 kpc which is very close to our estimation from the isochrone fitting method. Angelo et al. (2020), Cantat-Gaudin (2020), Kharchenko et al. (2013), and Tadross (2009) have been determined the distance value of IC 1434 as 3.1, 3.3, 3.2, and 3.0 kpc, respectively. Our derived value of distance is showing very good agreement with Angelo et al. (2020), Cantat-Gaudin (2020), and Kharchenko et al. (2013). The distance estimation of IC 1434 by Tadross (2009) is based on 2MASS and NOMAD data. Our obtained value of the distance is much precise than Tadross (2009) because our estimation is based on good quality optical data along with the high precision Gaia DR2 astrometry.

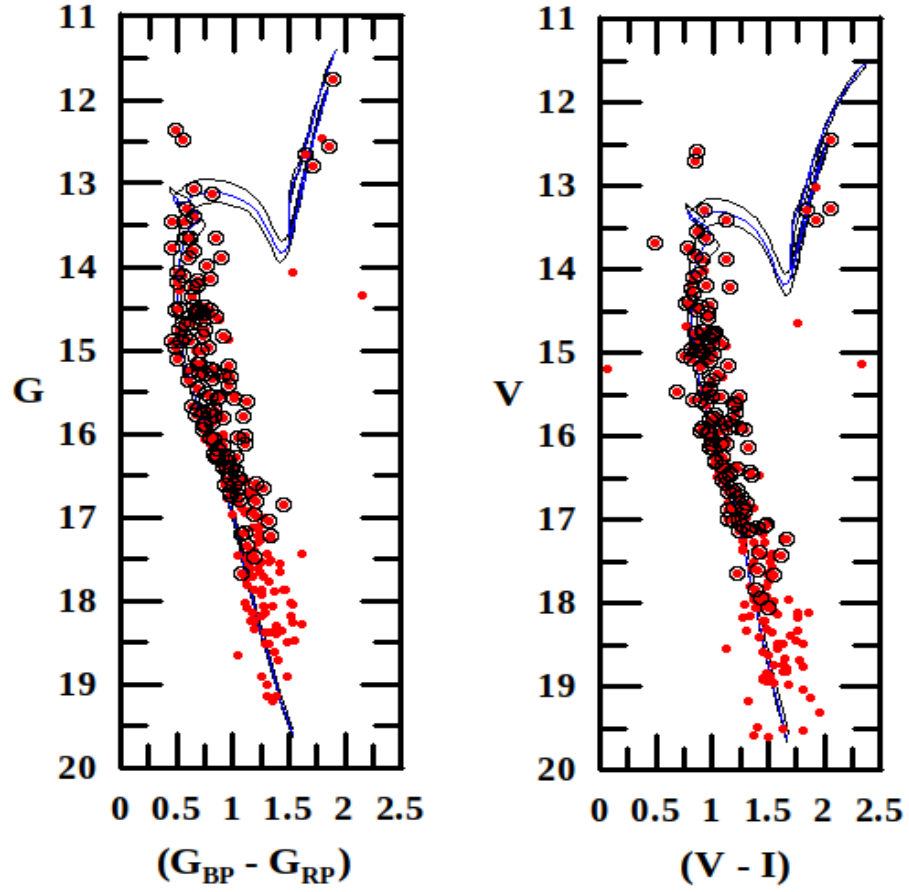


Fig. 12. Isochrone fitting to the CMDs. The curve is the solar metallicity isochrones taken from Marigo et al. (2017) of $(\log(\text{age}) = 8.75, 8.80, \text{ and } 8.85)$. The filled and open circles are our 238 members and 127 members of Cantat-Gaudin et al. (2018), respectively.

5. CONCLUSIONS

We presented the photometric and kinematic study of poorly studied open cluster IC 1434 using CCD *VRI* and Gaia DR2 data. We have estimated the membership probabilities of stars towards the region of IC 1434 and have found 238 members with a membership probability $\geq 60\%$. We have used those probable members to derive the fundamental parameters. The main results of the current investigation are as follows:

- The updated cluster center coordinates are estimated as: $\alpha = 332.612 \pm 0.06$ deg ($22^h 10^m 26.8^s$) and $\delta = 52.84 \pm 0.04$ deg ($52^\circ 50' 24''$) using the most probable cluster members. Cluster radii is obtained as 7.6 arcmin using radial density profile.
- On the basis of the vector point diagram and membership probability estimation of stars, we identified 238 most probable cluster members for IC 1434. The mean PMs of the cluster are estimated -3.89 ± 0.19 and -3.34 ± 0.19 mas yr $^{-1}$ in both the RA and DEC directions, respectively.
- Distance to the cluster IC 1434 is determined as 3.2 ± 0.1 kpc. This value is well supported by the distance estimated using mean parallax as 3.3 kpc. Age is estimated as 631 ± 73 Myr by comparing the cluster CMD with the theoretical isochrone given by Marigo et al. (2017) with $Z = 0.0152$.

6. ACKNOWLEDGEMENTS

The authors are thankful to the anonymous referee for useful comments, which improved the contents of the paper significantly. This work is supported by the IMHOTEP collaboration program No. 42088ZK between Egypt and France. D. Bisht is supported by the Natural Science Foundation of China (NSFC-11590782, NSFC-11421303). This work has made use of data from the European Space Agency (ESA) mission Gaia (<https://www.cosmos.esa.int/gaia>), processed by the Gaia Data Processing and Analysis Consortium (DPAC, <https://www.cosmos.esa.int/web/gaia/dpac/consortium>). Funding for the DPAC has been provided by national institutions, in particular the institutions participating in the Gaia Multilateral Agreement. This work has made use the TOPCAT <http://www.starlink.ac.uk/topcat>. It has been developed mostly in the UK within various UK and Euro-VO projects (Starlink, AstroGrid, VOTech, AIDA, GAVO, GENIUS, DPAC) and under PPARC and STFC grants. Its underlying table processing facilities are provided by the related packages STIL and STILTS. This research has made use of VizieR catalogue access tool, CDS, Aladin sky atlas developed at CDS, Strasbourg Observatory, France. This work has made use of data from the American Association of Variable Star Observers (AAVSO) Photometric All-Sky Survey (APASS) DR9 catalog.

7. REFERENCES

- Abdelaziz A.E., Hendy Y.H.M., Shokry A., et al., 2020, *Revista Mexicana de Astronomia y Astrofisica*, 56, 245
- Angelo M. S., Santos J. F. C., and Corradi W. J. B., 2020, *MNRAS*, 493, 3473
- Bisht D., Ganesh Shashikiran, Yadav R.K.S., et al., Geeta, 2018, *Adv. Space Res.*, 61, 517
- Bisht D., Yadav R.K.S., Ganesh Shashikiran., et al., 2019, *MNRAS*, 482, 1471B
- Bisht D., Zhu Qingfeng., Yadav R.K.S., et al., 2020a, *MNRAS*, 494, 607-623
- Bisht D., Elsanhoury W.H., Zhu Qingfeng, et al. 2020b, *AJ*, 160, 119B
- Bonatto C., and Bica E., 2009, *MNRAS* 397, 1915
- Cantat-Gaudin T., Jordi C., Vallenari A., et al., 2018, *A&A*, 618, 93
- Cantat-Gaudin T., Anders F., and Castro-Ginard A., 2020, *A&A*, 640A, 1C
- Chen L., Hou J.L., and Wang J.J., 2003, *AJ*, 125, 1397
- Dias W. S., Alessi B.S., Moitinho A, et al., 2002, *A&A*, 389, 873
- Friel, E. D., & Janes, K. A. 1993, *A&A*, 267, 75
- Friel E.D., 1995, *ARA&A*, 33, 381F
- Gaia Collaboration et al., 2016a, *A&A*, 595, A1
- Gaia Collaboration et al., 2016b, *A&A*, 595, A2
- Gaia Collaboration et al., 2018a, *A&A*, 616, A10
- Gaia Collaboration et al., 2018b, *A&A*, 616, A17
- Gao Xin-hua, 2018, *PASP*, 130, 124101
- Henden A., Munari U., 2014, *Contrib. Astron. Obs. Skalnat Pleso*, 43, 518
- Heden A., Templeton M., Terrell D., et al. 2016, *VizieR Online Data Catalog*, II/336
- Hendy Y.H.M., 2018, *NRIAG Journal of Astronomy and Geophysics*, 7, 180H
- Janes K., and Adler D., 1982, *ApJS*, 49, 425J
- Janes K.A., and Phelps R.L., 1994, *AJ*, 108, 1773J
- Jordi C., Gebran M., Carrasco J.M., et al., 2010, *A&A*, 523, A48
- Kharchenko N.V., Piskunov A.E., Roser S., et al., 2004, *Astron. Nachr.*, 325, 740
- Kharchenko N.V., Piskunov A.E., Schilbach E., et al., 2013, *A&A*, 558, A53
- King I., 1962, *AJ*, 67, 471
- Marigo P., Girardi L., Bressan A., et al., 2017, *ApJ*, 835, 77
- Maciejewski G., and Niedzielski A., 2007, *A&A*, 467, 1065
- Maciejewski G., and Niedzielski A., 2008, *Astron. Nachr.*, 329, 602
- Meynet G., Mermilliod J.-C., and Maeder A., 1993, *A&AS*, 98, 477M
- Monet David G., Levine Stephen E., Canzian Blaise, et al., 2003, *AJ*, 125, 984M
- Peterson C.J., and King I.R., 1975, *AJ*, 80, 427
- Phelps R. L., and Janes K.A., 1993, *AJ*, 106, 1870
- Rangwal G., Yadav R. K.S., Durgapal A., et al., 2019, *MNRAS*, 490, 1383

- Salgado J., Gonzalez-Nunez J., Gutierrez-Sanchez R., et al., 2017, A&C, 21, 22S
- Salpeter E.E., 1955, ApJ, 121, 161
- Sandage A., 1988, BAAS, 20, 1037S
- Spitzer L., and Hart M., 1971, ApJ, 164, 399
- Stetson P.B., 1980, AJ, 85, 387
- Stetson P.B., 1987, PASP, 99, 191
- Stetson P.B., 1992. In: Warrall, D.M., Biemesderfer, C., Barnes J., (Eds.), Astronomical Data Analysis Software and System I. ASP Conf. Ser. vol. 25, Astron. Soc. Pac., San Francisco, pp. 297
- Tadross A. L., 2009, New Astronomy, 14, 200
- Tadross A.L., and Hendy Y.H.M., 2016, Journal of the Korean Astronomical Society, 49, 57
- Tadross A.L., Bendary R., Hendy Y., et al., 2018, Astron. Nachr., 339, 698
- Twarog Bruce A., Ashman Keith M., and Anthony-Twarog Barbara J., 1997, AJ, 114, 2556T
- Vasilevskis S., Klemola A., and Preston G., 1958, AJ, 63, 387
- Yadav R.K.S., Sariya D.P., and Sagar R., 2013, MNRAS, 430, 3350
- Zhao J.L., and He Y.P., 1990, A&A, 237, 54